Development 137, 3257-3268 (2010) doi:10.1242/dev.053124

The ubiquitin proteasome system is required for cell proliferation of the lens epithelium and for differentiation of lens fiber cells in zebrafish

Fumiyasu Imai[1], Asuka Yoshizawa[1], Noriko Fujimori-Tonou[2], Koichi Kawakami[3] and Ichiro Masai[1,*]

SUMMARY

In the developing vertebrate lens, epithelial cells differentiate into fiber cells, which are elongated and flat in shape and form a multilayered lens fiber core. In this study, we identified the zebrafish *volvox* (*vov*) mutant, which shows defects in lens fiber differentiation. In the *vov* mutant, lens epithelial cells fail to proliferate properly. Furthermore, differentiating lens fiber cells do not fully elongate, and the shape and position of lens fiber nuclei are affected. We found that the *vov* mutant gene encodes Psmd6, the subunit of the 26S proteasome. The proteasome regulates diverse cellular functions by degrading polyubiquitylated proteins. Polyubiquitylated proteins accumulate in the *vov* mutant. Furthermore, polyubiquitylation is active in nuclei of differentiating lens fiber cells, suggesting roles of the proteasome in lens fiber differentiation. We found that an E3 ubiquitin ligase anaphase-promoting complex/cyclosome (APC/C) is involved in lens defects in the *vov* mutant. These data suggest that the ubiquitin proteasome system is required for cell proliferation of lens epithelium and for the differentiation of lens fiber cells in zebrafish.

KEY WORDS: Ubiquitin, Proteasome, Lens, Zebrafish, Psmd6, APC/C

INTRODUCTION

During development, the lens placode delaminates from the epidermal ectoderm and forms the lens vesicle. In the lens vesicle, posterior epithelial cells differentiate into lens fiber cells, whereas anterior epithelial cells are retained as proliferative lens progenitor cells (Bassnett et al., 1999; Lovicu and McAvoy, 2005). In zebrafish, a lens mass without a vesicle delaminates, and the cells reorganize into the central core and epithelial cells (Greiling and Clark, 2009). At the interface between the anterior lens epithelium and posterior lens fiber core, called the equator, epithelial cells differentiate into lens fiber cells, which elongate towards both anterior and posterior poles of the lens sphere and cover the old lens fiber core. In addition, lens fiber cells lose subcellular organelles, including the nucleus (Bassnett and Mataic, 1997), Golgi apparatus, endoplasmic reticulum (Bassnett, 1995) and mitochondria (Bassnett and Beebe, 1992). Previous studies have revealed regulatory factors involved in lens fiber cell differentiation. The transcription factor Pax6 is essential for lens placode induction (Ashery-Padan et al., 2000). Pax6 cooperates with several transcription factors, including Prox1 (Wigle et al., 1999), Pitx3 (Semina et al., 1998) and Foxe3 (Medina-Martinez and Jamrich, 2007). Foxe3 functions as a central factor in this regulatory network (Chow and Lang, 2001; Medina-Martinez and Jamrich, 2007) and regulates the expression of terminal differentiation genes, including that which encodes DNase II-like acid DNase (DLAD; Dnase2b). However, it is unclear how lens morphogenesis and organelle loss are related to these transcription factors.

The ubiquitin proteasome system (UPS) is important for the removal of unnecessary proteins and regulates normal cellular functions through the degradation of a variety of regulatory proteins (Nakayama and Nakayama, 2006; O'Connell and Harper, 2007). A cascade of enzymes, including ubiquitin-activating (E1), ubiquitin-conjugating (E2) and ubiquitin ligase (E3) enzymes, conjugate polyubiquitin to lysine residues in target proteins. Polyubiquitylated proteins are degraded by the 26S proteasome (Finley, 2009). The 26S proteasome is a ~2500 kDa complex consisting of one 20S core particle (CP) and two 19S regulatory particles (RPs) (Murata et al., 2009). Previous studies using in vitro cultures showed that the UPS is required for the proliferation of lens epithelial cells (Guo et al., 2006), mitochondrial degradation during lens fiber differentiation (Zandy and Bassnett, 2007), TGFβ-mediated lens fiber cell differentiation (Wu et al., 2007) and posterior capsular opacification (Hosler et al., 2006). It was reported that the UPS cooperates with a chaperone system to control protein quality (Bian et al., 2008; Bornheim et al., 2008). However, there have been a limited number of in vivo studies on the role of the UPS in lens fiber differentiation.

In zebrafish, lens development is similar to that of other vertebrates except that there is no formation of a lens vesicle. After 24 hours post-fertilization (hpf), differentiation of primary lens fiber cells begins, followed by formation of the anterior epithelium and the differentiation of secondary fibers from elongating epithelial cells near the equator. At 72 hpf, the lens grows to form a multilayered fiber core (Dahm et al., 2007; Greiling and Clark, 2009; Soules and Link, 2005). Genetic approaches have identified zebrafish mutants with defects in lens development (Fadool et al., 1997; Gross et al., 2005; Neuhauss et al., 1999; Vihtelic and Hyde, 2002). In this study, we describe a zebrafish mutant, *volvox* (*vov*), in which lens epithelial cells fail to maintain cell proliferation. Furthermore, lens fiber cells

[1]Developmental Neurobiology Unit, Okinawa Institute of Science and Technology (OIST), 1919-1 Azatancha, Onna, Okinawa 904-0412, Japan. [2]Initiative Research Program, Institute of Physical and Chemical Research (RIKEN), 2-1 Hirosawa, Wako, Saitama 351-0198, Japan. [3]Division of Molecular and Developmental Biology, National Institute of Genetics and Department of Genetics, Graduate University for Advanced Studies, 1111 Yata, Mishima, Shizuoka 411-8540, Japan.

*Author for correspondence (masai@oist.jp)

Accepted 16 July 2010

fail to fully elongate, and the number, shape and position of their nuclei are abnormal. The *vov* mutant gene encodes Psmd6, the RP subunit of the 26S proteasome, such that the mutation results in a reduction in proteasome activity. We found that an E3 ubiquitin ligase anaphase-promoting complex/cyclosome (APC/C) is implicated in *vov*-mediated lens defects. These data suggest that the UPS is required for cell proliferation of lens epithelium and for the differentiation of lens fiber cells in zebrafish.

MATERIALS AND METHODS

Fish

Zebrafish (*Danio rerio*) were maintained according to standard procedures (Westerfield, 1995). The RIKEN-wako (RW) and WIK strains were used as wild types for mutagenesis and mapping, respectively. Mutagenesis was performed as previously described (Masai et al., 2003). A *vov* mutant allele, *vov*^{rw619}, and a *p53* mutant allele, *tp53*^{M214K} (Berghmans et al., 2005), were used. SAGFF168A was identified as a zebrafish Tol2 transposon-mediated transgenic line that expresses a modified Gal4 in lens fiber cells (see Fig. S1 in the supplementary material) (Asakawa et al., 2008). The zebrafish Cecyil (cell cycle illuminated) transgenic line was used (see Fig. S1 in the supplementary material) (Sugiyama et al., 2009).

Mice

C57BL/6J mice were used. Embryos were fixed with 4% paraformaldehyde (PFA), dehydrated and embedded in paraffin wax.

Histology

Immunostaining of cryosections and paraffin sections, plastic sectioning and in situ hybridization were carried out as described previously (Imai et al., 2006; Masai et al., 2003). Paraffin sectioned slides were pretreated with heat (121°C, 5 minutes, in 10 mM citrate buffer pH 6.0). Nuclear staining was carried out using 1 μg/ml 4′,6-diamidino-2-phenylindole (DAPI; Sigma) or 1 nM TOPRO3 (Molecular Probes). Images were scanned under a LSM510 (Carl Zeiss) or FV1000 (Olympus) confocal laser-scanning microscope. Antibodies are described in Table 1. Terminal deoxynucleotide transferase-mediated dUTP nick-end labeling (TUNEL) was carried out using an In Situ Cell Death Detection Kit (Roche).

Incorporation of BrdU and EdU

Embryos were soaked in water containing 10 mM 5-bromo-2′-deoxyuridine (BrdU) or 1 mM ethynyl uridine (EdU) on ice for 15 minutes, rinsed, incubated for 30 minutes in water at 28.5°C and fixed with 4% PFA. Anti-BrdU labeling was carried out as described previously (Yamaguchi et al., 2005). EdU signals were detected using the Click-iT EdU Alexa Fluor Imaging Kit (Invitrogen).

Cell transplantation

Donor embryos were labeled at the one-cell stage with a 3-5% 1:1 mixture of FITC-dextran and biotin-dextran (Molecular Probes). Donor cells (5-10) were transplanted to host embryos at the late blastula stage. Host embryos carrying donor cells in the lens were selected by observing FITC fluorescence at 24 hpf, fixed with 4% PFA at 72 hpf and cryosectioned. Filamentous actin (F-actin) was stained using 0.1 μM Rhodamine-conjugated phalloidin (Molecular Probes).

Western blotting

Seventy-two hpf embryos were used for western blotting as described previously (Imai et al., 2006). An antibody against the N-terminal peptide sequence of zebrafish Psmd6 (amino acids 166-179) was generated using a synthetic peptide. Signals were developed using horseradish peroxidase (HRP)-conjugated secondary antibodies and Immobilon Western HRP substrate (Millipore). Luminescence was quantified using a Fuji LAS 4000 image analyzer (Fuji Photo Film). Antibodies are described in Table 1.

Construction of GFP-tagged Psmd6 and mKO-tagged Lamin A

GFP and monomeric Kusabira-Orange (mKO) were fused in frame to the N-terminus of the coding region of zebrafish *psmd6* (GenBank NM_200291) and *lamin A* (GenBank AF397016), respectively, and subcloned into the pCS2 vector (Rupp et al., 1994).

Morpholino antisense oligos (MOs)

MOs (Gene Tools) targeted against *psmd6* (*psmd6*-MO), *psmc2*-MO, *fzr1*-ATG-MO, *fzr1*-splicing-MO and their five-mismatch (5mis) MOs are described in Table S1 in the supplementary material. Because injection of *fzr1*-5misMO causes severe arrest of embryonic development during gastrulation, we confirmed that co-injection of *fzr1* RNA suppresses *fzr1* morphant defects (see Fig. S2 in the supplementary material).

Calculation of nuclear number, position and shape of lens fiber cells and lens fiber length

The numbers of lens fiber cell nuclei were counted on DAPI-labeled sections. The average and s.d. were determined using six lens images from three different embryos for each combination of genotypes, injections and stages. The percentage of lens fiber cell nuclei positioned in the anterior half of the lens sphere relative to the total number of lens fiber cell nuclei was calculated. Average and s.d. were determined using images of three sectioned lenses from different embryos. The maximum and minimum thickness of lens fiber cell nuclei were measured from images of lens sections and the ratio of the maximum to the minimum thickness was calculated for individual lens fiber cell nuclei using one image for each combination of genotypes, injections and stages. The length of individual lens fibers was measured on three-dimensional images, which were constructed by scanning GFP driven by the SAGFF168A transgenes. Averages were determined using nine lens fibers from two different wild-type embryos, eight lens fibers from two different *psmd6* morphant embryos and ten lens fibers from three different *fzr1* morphant embryos. Probabilities were determined by Student's *t*-test.

Table 1. Antibodies

Antibody	Dilution	Clone/company	Experiments
Polyubiquitylated protein	1:1000	Clone FK2; Millipore	Paraffin section/western blotting
AQP0	1:500	Millipore AB3071	Paraffin section
Prox1	1:100	Chemicon AB5475	Paraffin section
ZO-1	1:100	Clone ZO-1A12; Zymed	Paraffin section
Pcna	1:100	Clone PC10; Sigma	Paraffin section
Lamin B1	1:100	Abcam ab16048	Paraffin section
Pax6	1:100	Covance PRB-278P	Paraffin section
BrdU	1:100	Roche	Cryosection
Phosphorylated histone H3	1:1000	SC-8656; Santa Cruz	Cryosection
Zebrafish Psmd6	1:500	Generated by ourselves	Western blotting
Acetylated α-tubulin	1:1000	Clone 6-11B-1; Sigma	Western blotting
Rabbit HRP-conjugate IgG	1:2000	Goat; Amersham	Western blotting
Mouse HRP-conjugate IgG	1:2000	Goat; Amersham	Western blotting

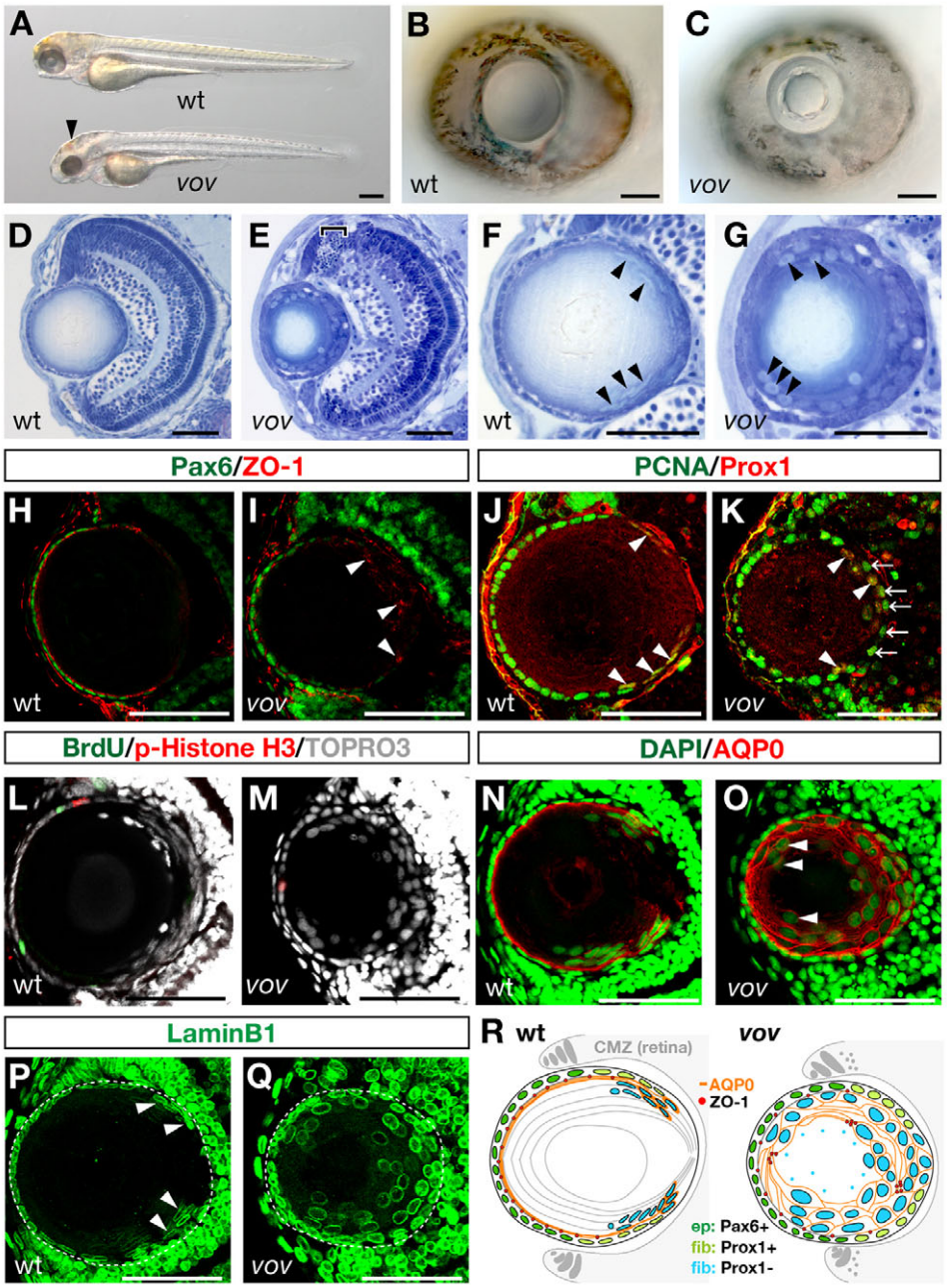

Fig. 1. Zebrafish *vov* mutant shows defects in lens fiber cell differentiation. (**A**) Wild-type (wt) and *vov* mutant 72 hpf embryos. The *vov* mutant embryos exhibit hemorrhaging on the roof of the mid-hindbrain (arrowhead). (**B**,**C**) Wild-type (B) and *vov* mutant (C) eyes at 72 hpf. (**D**,**E**) Sections of 72 hpf wild-type (D) and *vov* mutant (E) eyes. Bracket indicates apoptosis near the retinal ciliary marginal zone (CMZ) (E). (**F**,**G**) Wild-type (F) and *vov* mutant (G) lens. Nuclei are flat and positioned along the posterior edge of the wild-type lens sphere (arrowheads, F), whereas nuclei are swollen and located in the anterior region surrounding a small lens fiber core in the *vov* mutant (arrowheads, G). (**H**,**I**) Expression of Pax6 (green) and ZO-1 (red) in 72 hpf wild-type (H) and *vov* mutant (I) lens. Arrowheads indicate aggregated ZO-1 signals in the posterior lens region of the *vov* mutant. (**J**,**K**) Expression of Pcna (green) and Prox1 (red) in 72 hpf wild-type (J) and *vov* mutant (K) lens. Arrowheads indicate the Pcna and Prox1 double-positive cells. Arrows indicate Pcna-positive cells located in the posterior edge of the lens sphere (K), most of which weakly express Prox1 (see Fig. S3D-D‴ in the supplementary material). (**L**,**M**) Double labeling of 72 hpf wild-type (L) and *vov* mutant (M) lens with BrdU (green) and anti-pH3 antibody (red). Nuclei are stained with TOPRO3 (gray). (**N**,**O**) Expression of AQP0 (red) in 72 hpf wild-type (N) and *vov* mutant (O) lens. Nuclei are stained with DAPI (green). Arrowheads indicate nuclei of AQP0-positive lens fiber cells in the *vov* mutant, which are located in the anterior lens region (O). (**P**,**Q**) Expression of Lamin B1 in 72 hpf wild-type (P) and *vov* mutant (Q) lens. Arrowheads indicate wild-type lens fiber cell nuclei. White dashed lines indicate the outline of the lens sphere. (**R**) Schematic of wild-type and *vov* mutant lens. Lens epithelium (ep) expresses Pax6 (green) and its marginal cells are associated with retinal CMZ. After passing over the equator, lens epithelial cells transiently express Prox1 (light green) and differentiate into lens fiber cells (fib). Newly differentiating lens fiber cells (light blue) express AQP0 (orange) and their nuclei become flat and are subsequently denucleated. In the *vov* mutant, cell proliferation of lens epithelium is decreased and lens fiber cells are disorganized in morphology. ZO-1 signals are indicated by red circles. Anterior is left and dorsal is up in all the panels showing the lens (except in Fig. 3E,F and Fig. 6). Scale bars: 50 μm, except 250 μm in A.

Quantification of *psmd6* mRNA in wild type and *vov* mutant embryos

Total RNA was prepared from ten wild-type and ten *vov* mutant embryos at 72 hpf. Using an RNA LA PCR Kit (Takara Shuzo), *psmd6* and β-*actin* cDNA fragments were amplified from the same amount of wild-type and *vov* mutant cDNA in a series of PCR amplification cycles using gene-specific primers (see Table S2 in the supplementary material).

RESULTS

Zebrafish *vov* mutants display defects in lens fiber differentiation

We performed mutagenesis of zebrafish and identified a mutant, *vov*, which has a small lens core surrounded by less transparent, more irregularly shaped cells at 72 hpf (Fig. 1A-C). Cell death occurred near the ciliary marginal zone (CMZ) in the neural retina in the *vov* mutant (Fig. 1E; see Fig. S4H,J,L in the supplementary material). In the wild type, nuclei of lens fiber cells are flat and located in the posterior marginal region of the lens sphere at 72 hpf (Fig. 1F), whereas round-shaped nuclei were located not only in the posterior but also anterior marginal region surrounding a small transparent lens core in the *vov* mutant (Fig. 1G). We examined the expression of molecular markers at 72 hpf. Pax6 (Macdonald and Wilson, 1997) and *foxe3* (Shi et al., 2006) are expressed in the lens epithelium of zebrafish (Fig. 1H; see Fig. S3A-A″,E in the supplementary material). Both markers were observed in the lens epithelium of the *vov* mutant (Fig. 1I; see Fig. S3B-B″,F in the supplementary material). Proliferating cell nuclear antigen (Pcna) is a marker of the S phase and is normally expressed strongly in the lens epithelium and weakly in four or five cells that pass over the region adjacent to the retinal CMZ (Fig. 1J); these latter cells also express the early differentiation marker Prox1 (Glasgow and Tomarev, 1998) (see Fig. S3C-C‴ in the supplementary material). In the *vov* mutant, Pcna was expressed in the lens epithelium and in the cells located at the posterior edge of the lens sphere (Fig. 1K), and the latter mostly expressed Prox1 (see Fig. S3D-D‴ in the supplementary material), suggesting that lens fiber differentiation is initiated in the *vov* mutant. We examined cell proliferation in the lens epithelium by labeling with anti-phosphorylated histone H3 (pH3) antibody and BrdU incorporation. In the *vov* mutant, almost all lens epithelial cells were BrdU negative (Fig. 1L,M). The number of pH3-positive cells in the lens epithelium (n=0.26±0.14 per sectioned lens) was lower in *vov* mutants than in wild types (n=0.47±0.19), although the difference was not significant (P=0.198, t-test). These data suggest that the lens epithelium is specified normally in terms of the expression of Pax6 and *foxe3*, but that cell proliferation is slower or arrested in the *vov* mutant.

Next, we examined the structural integrity of the lens epithelium. Zonula occludens-1 (ZO-1; Tjp1 – Zebrafish Information Network) is a component of the tight and adherens junctions (Fanning and Anderson, 2009) and is localized at the apical surface of both lens epithelium and differentiating lens fiber cells (Kiener et al., 2007) (Fig. 1H; see Fig. S3A-A″ in the supplementary material). In the *vov* mutant, ZO-1 signals were observed beneath the lens epithelium, although they were weak and discontinuous at some points (Fig. 1I; see Fig. S3B-B″ in the supplementary material). Furthermore, aggregated ZO-1 signals were observed in the posterior region of the lens sphere in the *vov* mutant (Fig. 1I). Since the lens epithelium seemed to be maintained as a single sheet, discontinuous and aggregated ZO-1 signals in the *vov* mutant might be due to the disorganization of lens fiber cells. *alpha A crystallin* mRNA is expressed in differentiating lens fiber cells in wild-type zebrafish (see Fig. S3G in the supplementary material) (Kurita et al., 2003) and was similarly expressed beneath the lens epithelium in the *vov* mutant (see Fig. S3H in the supplementary material). Aquaporin-0 (AQP0; Mipa/b – Zebrafish Information Network) (Shiels and Bassnett, 1996) is expressed in newly differentiating lens fiber cells in the wild type, which surround the AQP0-negative old lens fiber core (Fig. 1N). In the *vov* mutant, AQP0 expression was observed in lens cells, which were not tightly packed and surrounded a small AQP0-negative core (Fig. 1O). Lamin B1 demarcates nuclear membranes in zebrafish (Collas, 1999). After cell cycle exit, lens fiber nuclei become flat and are arranged along the posterior rim of the lens sphere in the wild type (Fig. 1P), whereas lens nuclei were not flat and were located in the marginal region of the entire lens in the *vov* mutant (Fig. 1Q). These data suggest that lens fiber cell differentiation is initiated but nuclear position and shape are disorganized in the *vov* mutant (Fig. 1R).

We examined apoptosis by TUNEL. There was no TUNEL signal in the wild-type lens at 48, 72 and 96 hpf (see Fig. S4A,C,E in the supplementary material), suggesting that TUNEL does not detect lens denucleation in zebrafish by 96 hpf. In the *vov* mutant, there was no TUNEL signal at 48 hpf (see Fig. S4B in the supplementary material), but dot-like TUNEL signals were observed around the central lens fiber core at 72 hpf (see Fig. S4D in the supplementary material), and strong TUNEL signals were observed in cells surrounding the small lens fiber core at 96 hpf (see Fig. S4F in the supplementary material). These data suggest that lens nuclei are degraded in the *vov* mutant after 72 hpf, but possibly not by a normal process of denucleation.

Generation of lens fiber cells is compromised in the *vov* mutant

We examined cell proliferation in lens epithelium by EdU incorporation. Here we defined Pax6-positive lens cells as epithelial cells with the margin associated with the retinal CMZ (Fig. 1H; Fig. 2A, red cells). In wild-type epithelium, 30-40% of cells were labeled with EdU from 36 to 72 hpf (Fig. 2B-E), whereas the percentage of EdU incorporation decreased at 48 hpf (Fig. 2F,G) and was almost zero at 60 and 72 hpf (Fig. 2H,I) in the *vov* mutant. These data suggest that cell proliferation becomes slower or arrested and ceases after 60 hpf in the *vov* mutant (Fig. 2L). Next, we examined the number of nuclei of lens fiber cells. We defined Pax6-negative lens cells as lens fiber cells (Fig. 2A, green cells) and counted their nuclear number on lens sections cut along the optic axis. In wild types, the number of lens fiber nuclei increased and peaked at 48 hpf, maintained a plateau from 48 to 60 hpf, and decreased at 72 hpf (Fig. 2J,M). The plateau between 48 and 60 hpf suggests that the number of newly generated lens cells is nearly equal to the number of lens nuclei degraded by denucleation. In the *vov* mutant, the number of lens fiber cell nuclei was lower than in wild type at 36 and 48 hpf (Fig. 2K,M), suggesting a reduced generation rate of lens fiber cells. In contrast to the wild type, the number of lens fiber cell nuclei continued to increase after 48 hpf and reached wild-type levels at 60 hpf in the *vov* mutant (Fig. 2M). The increase of lens fiber cell nuclei between 48 and 60 hpf in the *vov* mutant suggests that the number of lens fiber cells generated is higher than the number of lens nuclei degraded by denucleation. From 60 to 72 hpf, the number of lens fiber nuclei decreased in the *vov* mutant (Fig. 2M). Because there was no production of lens fiber cells after 60 hpf in the *vov* mutant (Fig. 2L), this reduction of lens nuclei seems to be due to the loss of lens fiber cell nuclei, which may be detected by TUNEL (see Fig. S4D,F in the supplementary material).

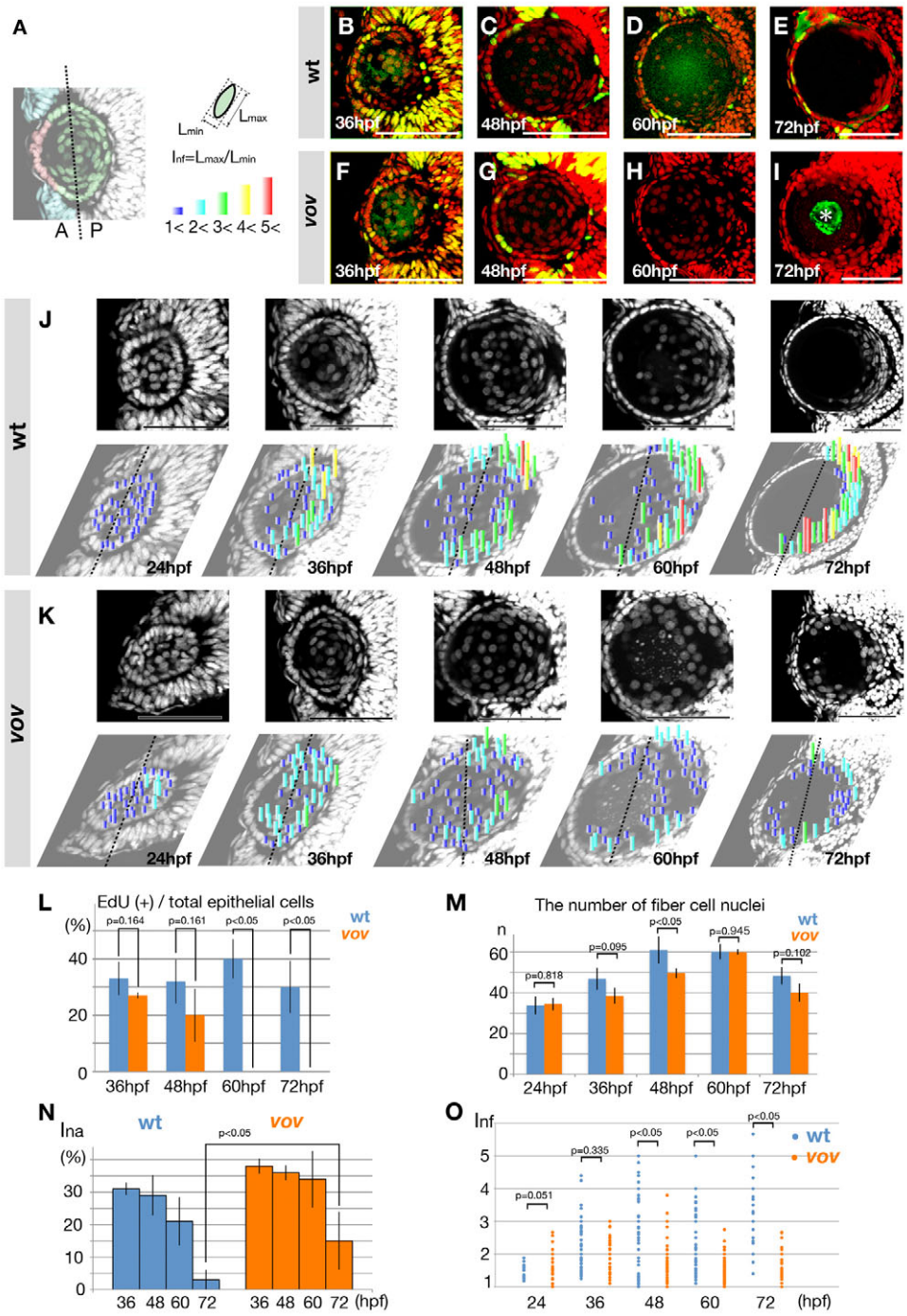

Fig. 2. The shape, position and nuclei number of lens fiber nuclei are affected in the *vov* mutant. (**A**) Color key for lens epithelial cells and lens fiber cells. From 36 to 72 hpf, the margin of Pax6-positive lens epithelium (red) is associated with the retinal CMZ (light blue). Lens fiber cells are defined as Pax6-negative lens cells (green). The interface between the anterior and posterior half of the lens sphere is indicated by a dotted line. Index of nucleus flatness (Inf) is calculated as the ratio of the maximum (L_{max}) to the minimum (L_{min}) nuclear thickness. Inf=1.0-2.0, dark blue; 2.0-3.0, light blue; 3.0-4.0, green; 4.0-5.0, yellow; more than 5.0, red. (**B-I**) EdU incorporation (green) and DAPI labeling (red) of wild-type (B-E) and the *vov* mutant (F-I) zebrafish lens. Asterisk shows non-specific EdU signals (I). (**J**,**K**) Nuclear staining (upper panels) of wild-type (J) and the *vov* mutant (K) lens with DAPI. Inf is plotted to individual nuclei of lens fiber cells on the lower row of images. The degree of flatness is indicated by the height of bars and their color (see A). Dotted lines indicate the interface between the anterior and posterior halves. (**L**) The percentage of EdU-positive cells relative to the total number of lens epithelial cells in wild type (light blue bars) and the *vov* mutant (red bars). (**M**) The number of lens fiber cell nuclei in the wild type (light blue bars) and *vov* mutant (red bars). (**N**) Index of nuclear anterior localization (Ina) of the wild type and *vov* mutant. (**O**) The Inf of individual lens fiber cell nuclei in the wild type and *vov* mutant. Scale bars: 50 μm.

Nuclear position and shape of lens fiber cells are affected in the *vov* mutant

We next examined the position of lens fiber cell nuclei. Sectioned lenses cut along the optic axis were divided into anterior and posterior halves (Fig. 2A). The percentage of lens fiber nuclei positioned in the anterior half relative to the total number of lens fiber cell nuclei was defined as the index of nuclear anterior localization (Ina) (Fig. 2J,K,N). In wild types, Ina was ~30% at 36 and 48 hpf, decreased to 20% at 60 hpf and 3% at 72 hpf (Fig. 2N), suggesting that 97% of lens fiber cell nuclei were positioned in the posterior half of the lens sphere at 72 hpf. However, in the *vov* mutant, Ina was greater than 30% until 60 hpf and decreased to 15% at 72 hpf, which is higher than that of wild types. These observations suggest that a significant number of lens nuclei are positioned in the anterior half of the lens sphere in the *vov* mutant.

Next, we examined the shape of lens fiber cell nuclei. To determine their flatness, we measured the maximum and minimum thickness of lens fiber cell nuclei and calculated the ratio of the maximum to the minimum thickness as the index of nucleus flatness (Inf) (Fig. 2A). In wild types, Inf varied from 1.0 to 2.0 at 24 hpf, from 1.0 to 4.5 at 36 hpf, and from 1.0 to greater than 5.0 after 48 hpf (Fig. 2O), indicating that the maximum value of Inf increases as development proceeds. Lens nuclei with a higher value of Inf were more posteriorly positioned in the lens sphere (Fig. 2J,

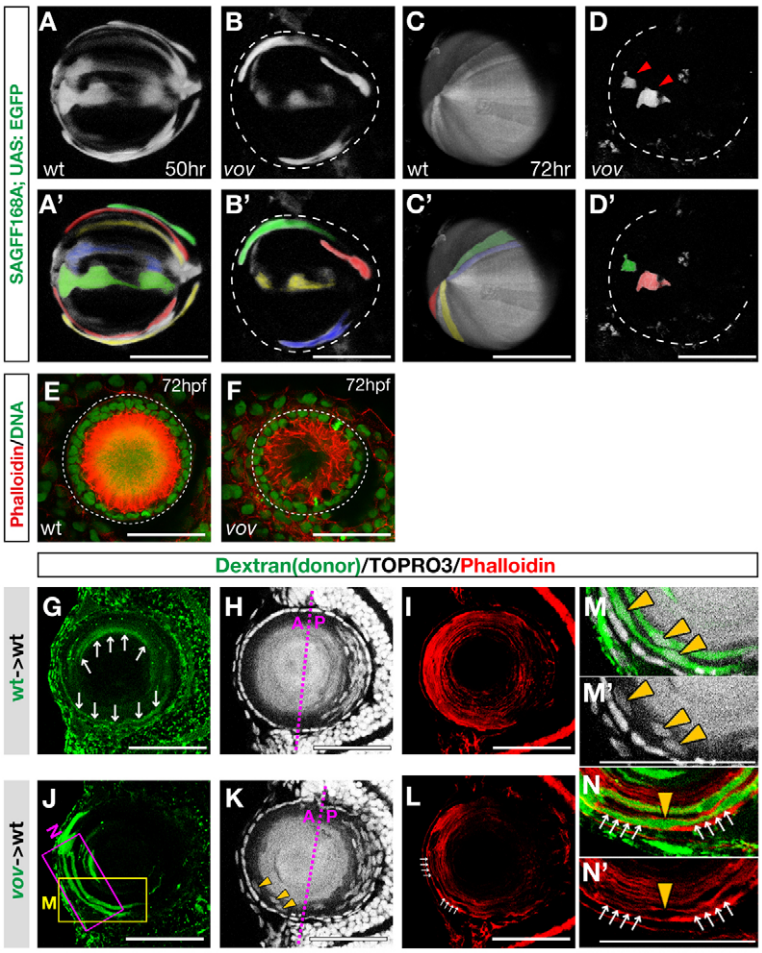

Fig. 3. Morphogenesis of lens fiber cells is affected in the *vov* mutant. (**A-D'**) Confocal images of the lens of 50 hpf wild type (A) and *vov* mutant (B) and 72 hpf wild type (C) and *vov* mutant (D) zebrafish expressing the SAGFF168A; UAS:EGFP transgenes. Individual lens fiber cells are indicated by pseudocolors (A'-D'). In the *vov* mutant, GFP-expressing cells do not maintain a fiber-like structure and appear to undergo degradation (D, arrowheads). (**E**,**F**) Anterior view of 72 hpf wild-type (E) and the *vov* mutant (F) lens labeled with Rhodamine-conjugated phalloidin (red) and Sytox Green (green). (**G-N'**) Transplantation of wild-type (G-I) and *vov* mutant (J-N) donor cells into wild-type recipient lens. Labeling is with biotin-dextran (green) (G,J), TOPRO3 (gray) (H,K) and phalloidin (red) (I,L). (M,N) High magnification of the boxed regions shown in J. Wild-type donor cells transplanted into wild-type recipient lens elongate to be very thin, resulting in weak signals (arrows, G). Nuclei of *vov* mutant donor lens fiber cells were frequently positioned in the anterior lens fiber region (yellow arrowheads, K,M,M') and F-actin density is lower in the *vov* mutant (white arrows, L,N,N'). Scale bars: 50 μm.

lower panels). In a majority of lens fiber cell nuclei of the *vov* mutant, Inf was less than 3.0 at all stages examined (Fig. 2K,O), suggesting that the nuclei of lens fiber cells fail to flatten. Electron microscopy analyses confirmed the defects in nuclear position and shape of lens fiber cells in the *vov* mutant (see Fig. S5 in the supplementary material). Furthermore, we found that retinal apoptosis in the *vov* mutant was inhibited by a genetic mutation of the tumor suppressor *p53* (*tp53*) (Berghmans et al., 2005) (see Fig. S6DL in the supplementary material). However, the proliferation of lens epithelial cells and the nuclear position and shape of lens fiber cells were affected in the *vov*; *p53* double mutant (see Fig. S6H,V,W in the supplementary material). It seems likely that retinal apoptosis is not a primary cause of *vov*-mediated lens defects (see Fig. S6 in the supplementary material).

Morphogenesis of lens fiber cells is affected in the *vov* mutant

To visualize individual lens fiber cells, we used a zebrafish transgenic line SAGFF168A; UAS:EGFP, in which GFP is expressed in differentiating lens fiber cells. At 50 hpf, GFP-positive lens fiber cells elongate toward the anterior and posterior poles of the lens sphere (Fig. 3A). At 72 hpf, most lens fiber cells express GFP and their apical tips converge at one point at the anterior pole of the wild-type lens sphere (Fig. 3C). In the *vov* mutant, lens fiber cells were shorter than in the wild type at 50 hpf (Fig. 3B), and markedly smaller at 72 hpf (Fig. 3D), suggesting that the *vov* mutant lens fiber cells do not fully elongate. Actin filament bundles develop during the differentiation of lens fiber cells (Bassnett et al., 1999; Lee et al., 2000). Filamentous actin (F-actin) was densely labeled with phalloidin in the wild-type lens fiber region (Fig. 3E), whereas F-actin density was sparse in the *vov* mutant (Fig. 3F).

Next, we carried out cell transplantation at the blastula stage. When wild-type donor cells were incorporated into the wild-type recipient lens, the donor lens cells differentiated into flat and elongated lens fiber cells (Fig. 3G), their nuclei were observed in the posterior half of the lens sphere at 72 hpf (Fig. 3H), and F-actin accumulated in differentiating lens fiber cells (Fig. 3I). When the *vov* mutant donor cells were incorporated into the wild-type recipient lens, the *vov* mutant donor cells seemed to differentiate into lens fiber cells that were thicker than wild-type donor cells (Fig. 3J), and their nuclei were frequently positioned in the anterior half of the lens sphere (n=7 from three lenses) (Fig. 3K,M,M′, yellow arrowheads). F-actin density was decreased in the *vov* mutant donor lens fiber cells (n=5 from three lenses) (Fig. 3L,N,N′, white arrows). These data suggest that the *vov* mutation cell-autonomously compromises the elongation of lens fiber cells, their nuclear position and F-actin assembly.

The *vov* mutant gene encodes a subunit of the proteasome

We mapped the genetic locus of the *vov* mutation between two polymorphic markers, zK22H2 and zK251M8, at 39.3 cM on chromosome 11 (see Fig. S7A in the supplementary material), and sequenced cDNAs of candidate genes. We found that the *vov* gene encodes Psmd6, a RP subunit of the proteasome. In the *vov* mutant

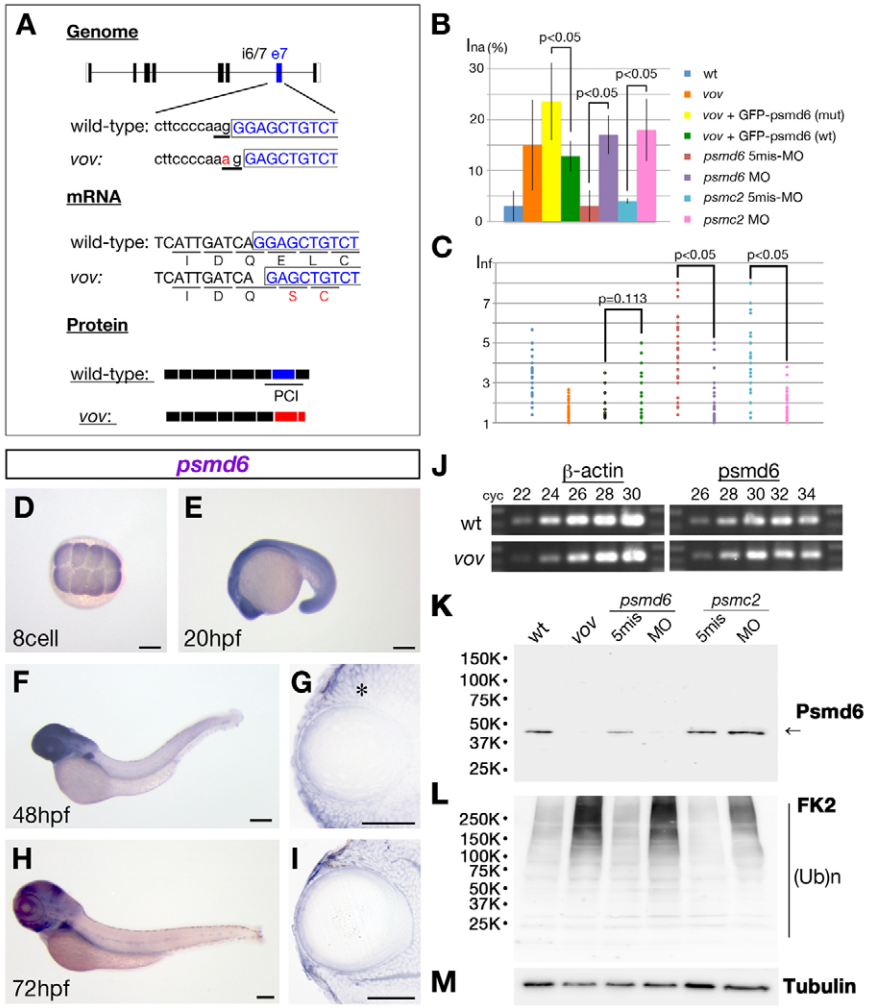

Fig. 4. The *vov* mutant gene encodes Psmd6. (**A**) Nucleotide substitution from G to A occurs in a splicing acceptor site of the intron6/7-exon7 boundary (top, underlined), causing a one-base deletion in the *psmd6* mRNA that results in a frameshift within the coding region (middle panel) and loss of the PCI domain (bottom panel). (**B**,**C**) Ina (B) and Inf (C) of wild type, *vov* mutant, *vov* mutant injected with GFP-tagged *psmd6* RNA carrying the *vov* mutation, *vov* mutant injected with wild-type GFP-tagged *psmd6* RNA, *psmd6* and *psmc2* morphants and their five-mismatch morphants. Ina is lower and the maximum value of Inf is higher in the *vov* mutant injected with wild-type GFP-tagged-*psmd6* RNA (green) than in the *vov* mutant injected with GFP-tagged-*psmd6* RNA carrying the *vov* mutation (yellow), suggesting that wild-type *psmd6* RNA injection rescues the *vov*-mediated defects in nuclear position and shape of lens fiber cells. Ina is higher and the maximum value of Inf is lower in *psmd6* (purple) and *pmsc2* morphants (pink) than in their five-mismatch morphants (brown and light blue), suggesting that these MOs induce the *vov*-like lens defects. (**D-I**) Expression of zebrafish *psmd6* mRNA at the eight-cell stage (D) and at 20 (E), 48 (F,G) and 72 hpf (H,I). (G,I) Plastic sections of eyes. Asterisk indicates *psmd6* expression in the retinal CMZ. (**J**) Semi-quantitative PCR of wild type and *vov* mutant at 72 hpf using *psmd6* and β-*actin* gene primers. The number of PCR cycles is indicated above each lanes. (**K-M**) Western blotting of 72 hpf wild type, *vov* mutant, *psmd6* and *psmc2* morphants and their five-mismatch morphants with anti-zebrafish Psmd6 (K), anti-polyubiquitylated protein (FK2) (L) and anti-acetylated α-tubulin (M, a loading control). The level of Psmd6 (arrow) is reduced in the *vov* mutant and *psmd6* morphant, but is unaffected in the *psmc2* morphant (K). The levels of polyubiquitylated proteins increase in the *vov* mutant, *psmd6* and *psmc2* morphant (K). Scale bars: 250 μm in D-F,H; 50 μm in G,I.

genome, a G-to-A substitution occurred at the splice acceptor site prior to the seventh exon of *psmd6*, resulting in a single base shift of the splice acceptor site (Fig. 4A, top). This one-base deletion of cDNA causes a frameshift in the coding region, resulting in the loss of the proteasome-COP9-initiation factor (PCI) domain, which is required for proteasome activity (Sha et al., 2007) (Fig. 4A, bottom). Next, we carried out RNA-mediated rescue and MO-mediated knockdown experiments. Injection of GFP-tagged *psmd6* RNA into *vov* mutant embryos suppressed retinal cell death (see Fig. S8 in the supplementary material) and lens defects at 72 hpf (Fig. 4B,C; see Fig. S7C,G in the supplementary material). The injection of *psmd6*-MO induced the *vov*-like lens defects (Fig. 4B,C; see Fig. S7E,I in the supplementary material). These data suggest that the *vov* mutant gene encodes Psmd6.

Reduction in proteasome activity causes the *vov*-mediated lens defects

We next examined *psmd6* mRNA expression. *psmd6* mRNA was ubiquitously expressed at the eight-cell stage, suggesting maternal expression (Fig. 4D). The expression was observed ubiquitously at 20 hpf (Fig. 4E), and was prominent in the head at 48 (Fig. 4F) and 72 (Fig. 4H) hpf. *psmd6* mRNA was expressed in the anterior lens

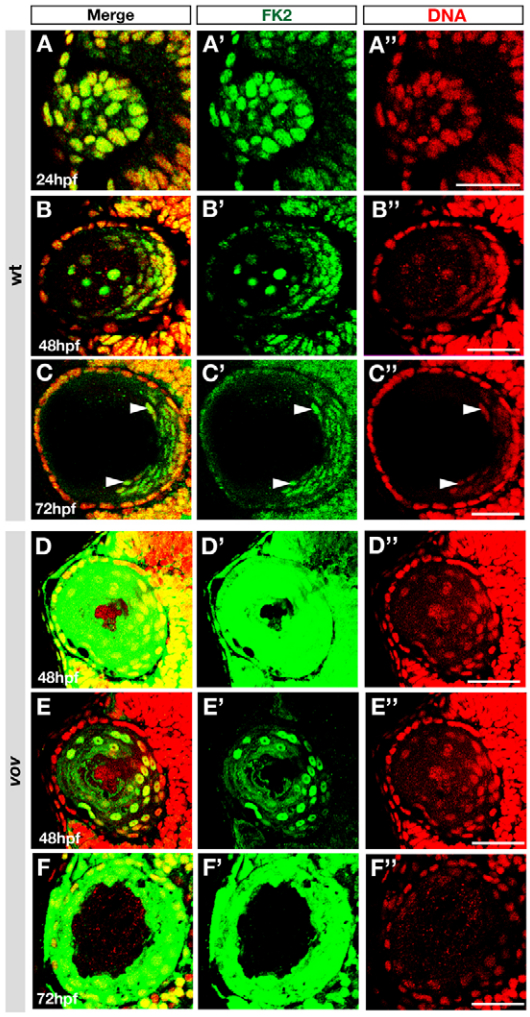

Fig. 5. Polyubiquitylated proteins are localized in lens fiber cell nuclei. (**A-F**) Labeling of wild-type (A-C) and *vov* mutant (D-F) zebrafish lens of the indicated stages with anti-polyubiquitylated protein antibody (FK2, green) and TOPRO3 (red). Arrowheads indicate signals in nuclei of differentiating lens fiber cells at 72 hpf (C). Scanning conditions of images in D,F were the same as those for B,C. (E) The same image as D but with reduced sensitivity of fluorescence detection. (**A′-F′**,**A″-F″**) The same images as A-F but shown through a green (FK2) or red (TOPRO3) channel. Scale bars: 50 μm.

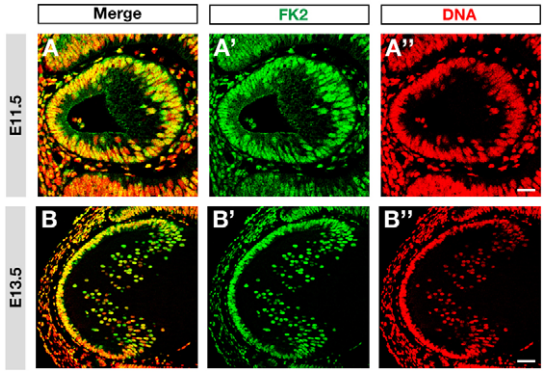

Fig. 6. Labeling of mouse lens with anti-polyubiquitylated protein antibody. (**A**,**B**) Labeling of mouse lens with anti-polyubiquitylated protein FK2 (green) and TOPRO3 (red). At 11.5 (A), lens delaminates to form a vesicle and primary fibers start to elongate. At 13.5 (B), lens epithelial cells cover the lens sphere anteriorly, differentiate into lens fiber cells at the equatorial region and elongate anteriorly to fill the hollow lens vesicle. FK2 signals are observed in nuclei of lens epithelial cells and lens fiber cells. (**A′**,**B′**,**A″**,**B″**) The same images as A,B but shown through a green (FK2) and red (TOPRO3) channel. Scale bars: 50 μm.

epithelium and retinal CMZ (Fig. 4G,I), suggesting that *psmd6* mRNA is expressed in proliferating cells and early differentiating cells in both the lens and retina. Semi-quantitative PCR revealed that the mRNA level in the *vov* mutant was similar to that of the wild type (Fig. 4J). Western blotting, using an anti-zebrafish Psmd6 antibody, revealed a single band of 44 kDa, which is identical to the molecular weight of Psmd6 (Fig. 4K). This band decreased in both the *vov* mutant and *psmd6* morphant at 72 hpf (Fig. 4K), suggesting that the level of Psmd6 protein is reduced in both cases.

A yeast homolog of *psmd6*, *rpn7*, is required for proteasome activity (Isono et al., 2007; Isono et al., 2004; Sha et al., 2007). We examined the level of polyubiquitylation in the *vov* mutant and *psmd6* morphant by western blotting using the anti-polyubiquitylated protein antibody FK2 (Fujimuro et al., 1994). Polyubiquitylated proteins accumulated in both the *vov* mutant and the *psmd6* morphant at 72 hpf (Fig. 4L), suggesting that proteasome-dependent protein degradation is compromised in both cases. Furthermore, we injected an MO for *psmc2* (*rpt1* in yeast), which encodes another RP subunit of the proteasome, into wild-type embryos. The *psmc2* morphant showed an increase in polyubiquitylation at 72 hpf (Fig. 4L) and lens defects similar to those of the *vov* mutant and *psmd6* morphant (Fig. 4B,C; see Fig. S7J-N in the supplementary material). These data suggest that the reduction of proteasome activity correlates with lens defects in the *vov* mutant.

The UPS is active in the nucleus of lens fiber cells

Using the anti-polyubiquitylated protein antibody FK2, we examined the spatiotemporal pattern of polyubiquitylation in the zebrafish lens. At 24 hpf, signals were detected in nuclei of wild-type lens cells (Fig. 5A). At 48 hpf, signals were weaker in nuclei of lens epithelial cells, but were maintained at high levels in the nuclei of differentiating lens fiber cells (Fig. 5B). At 72 hpf, signals were detected in nuclei of differentiating lens fiber cells (Fig. 5C, arrowheads). In the *vov* mutant, the expression levels of polyubiquitylated proteins increased (Fig. 5D-F). The antibody signals nearly reached saturation level in the *vov* mutant, and signals were high in lens fiber cell nuclei (Fig. 5E). These observations suggest that polyubiquitylated proteins accumulate in the nucleus of zebrafish lens fiber cells. We also found that polyubiquitylated proteins accumulated in the nuclei of lens epithelium and lens fiber cells in the mouse (Fig. 6A,B).

We examined the localization of Psmd6 in the zebrafish lens using the anti-Psmd6 antibody used for western blotting (Fig. 4K). However, we were unable to detect specific signals by immunohistolabeling (data not shown). Because the GFP-tagged Psmd6 suppressed lens defects in the *vov* mutant (Fig. 4B,C), the GFP-tagged Psmd6 was considered to be functional. Thus, we injected RNA encoding the GFP-tagged Psmd6 into wild-type embryos and examined its expression pattern. GFP signals were detected throughout the lens cells at 24 hpf (Fig. 7A), but localization was restricted to nuclei of lens fiber cells at 33 (Fig.

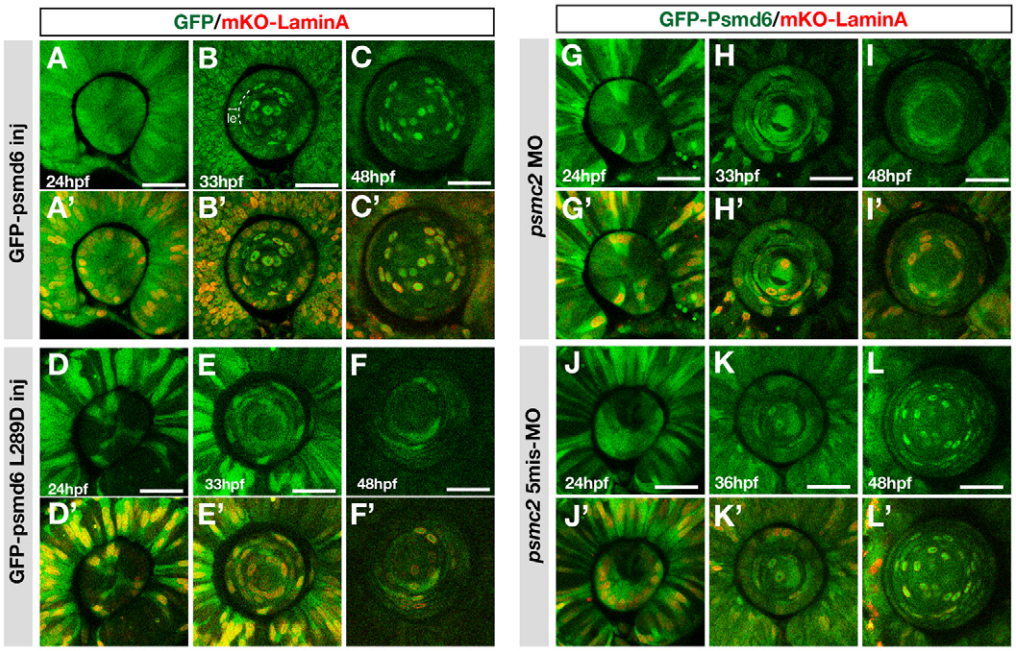

Fig. 7. Localization of GFP-tagged Psmd6 in lens fiber cell nuclei. (**A-F′**) Localization of GFP-tagged Psmd6 (green) (A-C) and GFP-tagged Psmd6 carrying the L289D mutation (green) (D-F) in wild-type zebrafish lens of the indicated stages. Nuclear membranes are visualized with mKO-Lamin A (red) (A′-F′). le, lens epithelial region. (**G-L′**) Localization of GFP-tagged Psmd6 in *psmc2* morphant (G-I) and *psmc2* five-mismatch morphant (J-L) lens. Nuclear membranes are visualized with mKO-Lamin A (red) (G′-L′). All panels are anterior views of the lens sphere. Scale bars: 50 μm.

7B) and 48 (Fig. 7C) hpf. The intensity of GFP in the lens epithelial nuclei was weaker than that of lens fiber cells at 33 and 48 hpf. These localization patterns were similar to those of polyubiquitylated proteins (Fig. 5A-C).

To confirm whether the nuclear localization of GFP-tagged Psmd6 is related to proteasome function, we carried out two sets of experiments. First, we examined the subcellular localization of GFP-tagged Psmd6 carrying an amino acid substitution, L289D, which compromises the assembly of Psmd6 into the proteasome complex (Sha et al., 2007). GFP-tagged Psmd6 with the L289D mutation was localized to the nuclei of lens fiber cells less efficiently than GFP-tagged wild-type Psmd6 (Fig. 7D-F). Second, we examined the localization of GFP-tagged Psmd6 in the *psmc2* morphant lens. GFP-tagged Psmd6 was not localized efficiently to lens fiber nuclei in the *psmc2* morphant (Fig. 7G-I). These data suggest that the nuclear localization of GFP-tagged Psmd6 depends on proteasome function.

APC/C is required for lens fiber differentiation

APC/C regulates the G2/M phase transition in the cell cycle (Pesin and Orr-Weaver, 2008; Peters, 2006) and the morphogenesis of differentiating neurons (Konishi et al., 2004; Stegmuller et al., 2008). APC/C inhibition causes a decrease in the number of lens fibers in the mouse (Wu et al., 2007). We focused on one of the APC/C targets, Geminin (McGarry and Kirschner, 1998). To monitor the APC/C-dependent degradation of Geminin, we used Cecyil transgenic zebrafish, which express monomeric Kusabira-Orange 2-tagged zebrafish Cdt1 N-terminal 190 amino acid domain (mKO2-zCdt1) and monomeric Azami-Green-tagged zebrafish Geminin N-terminal 100 amino acid domain (mAG-zGem) (Sugiyama et al., 2009). In the Cecyil transgenic line, mAG-zGem expression was detected only in lens epithelial cells at 48 hpf (Fig. 8A), whereas mKO2-zCdt1 expression was detected in lens fiber cells (Fig. 8A′). In the *psmd6* morphants, mAG-zGem was detected ectopically in lens fiber cells, which were mKO2-zCdt1 positive (Fig. 8B′), suggesting that APC/C-dependent protein degradation is compromised in the *psmd6* morphant. Fzr1 (Cdh1) is a coactivator of APC/C (Pesin and Orr-Weaver, 2008; Peters, 2006). We examined the lens phenotypes of zebrafish *fzr1* morphants. In the *fzr1* morphant lens, mAG-zGem was retained in mKO2-zCdt1-positive lens fiber cells (Fig. 8C′,D′). Furthermore, rounded nuclei of lens fiber cells were positioned throughout the entire region of the lens sphere (Fig. 8E). Similar to the *vov* mutant, cell proliferation was affected, but lens epithelium and lens fiber cells were specified in terms of Pax6 and AQP0 expression in the *fzr1* morphant lens (see Fig. S9 in the supplementary material). The maximum value of Inf was lower in the severe *fzr1* morphants than in wild types (Fig. 8H). Furthermore, Ina was higher in the *fzr-1* morphants than in wild types (Fig. 8I). There was no TUNEL signal in the *fzr1* morphant lens (Fig. 8F,G). Finally, lens fiber cells did not elongate fully in the *fzr1* morphant (Fig. 8J-M).

DISCUSSION

The UPS is required for lens epithelial cell proliferation

Proliferation and differentiation are tightly controlled in the vertebrate lens (Lovicu and McAvoy, 2005). It has been reported that the application of proteasome inhibitors suppresses the proliferation of lens epithelial cells (Guo et al., 2006; Liu et al., 2006). In *vov* mutants, lens epithelial cells are specified normally in terms of the expression of *pax6* and *foxe3* but fail to maintain cell proliferation. Our findings provide in vivo evidence that the UPS is required for cell cycle control in the vertebrate lens epithelium. In the *vov* mutant, the number of lens epithelial cells in the S phase is reduced at 48 hpf and they are almost absent after 60 hpf. However, pH3-positive lens epithelial cells and Prox1-positive early differentiating lens fiber cells appear in the *vov* mutant at 72 hpf, although the number of pH3-positive cells is lower in the *vov* mutant than in the wild type. How is cell cycle control affected in the *vov* mutant? The first possibility is that lens epithelial cells are arrested in G1 phase and do not enter S phase after 60 hpf. In this case, lens epithelial cells that exit from the S phase by 60 hpf may continue to undergo the G2/M phase, and some of them may differentiate into lens fiber cells at 72 hpf. The second possibility is that cell cycle arrest or stalling occurs in the intra-S, G2 or late M phase. Further studies will be necessary to address this issue.

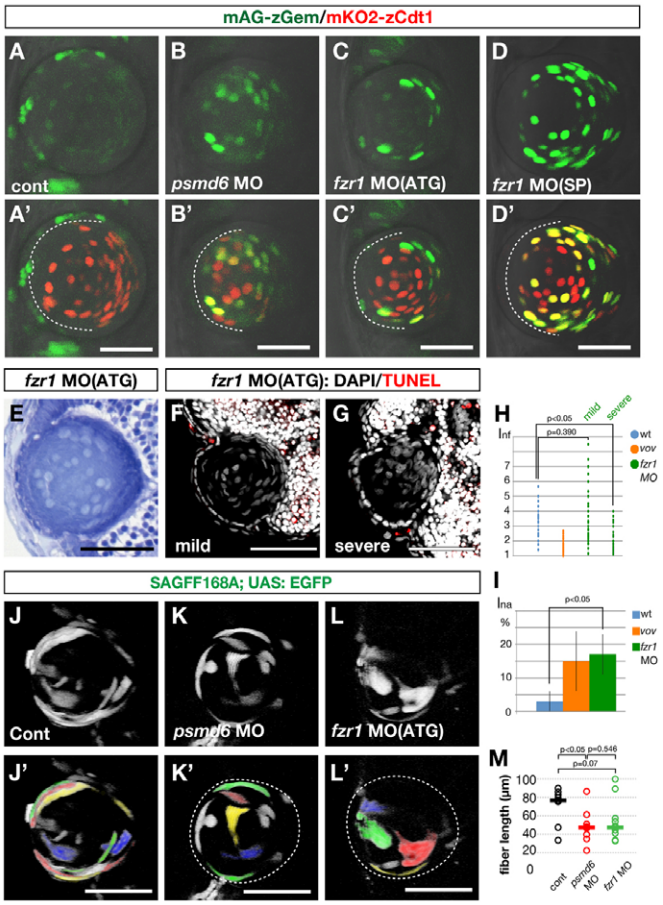

Fig. 8. APC/C is required for lens fiber differentiation. (**A-D'**) Confocal images of 48 hpf wild type (A'), *psmd6* morphant (B'), *fzr1* ATG-morphant (C') and *fzr1* splicing-morphant (D') zebrafish lens in the Cecyil transgenic background. (A-D) Green channel (mAG-zGem) only. Dashed lines indicate the interface between the lens epithelium and lens fiber core. mAG-zGem and mKO2-zCdt1 (red) expression overlap in the lens fiber cells of *psmd6* and *fzr1* morphants. mAG-zGem (green) expression is absent in the epithelium of *psmd6* (B') and *fzr1* (C',D') morphant lens. The reduction of mAG-zGem seems to correlate with the absence of BrdU/EdU incorporation (Fig. 2L and see Fig. S9 in the supplementary material). (**E**) Lens of 72 hpf *fzr1* morphant. (**F**,**G**) TUNEL (red) and DAPI (gray) labeling of 72 hpf lens of mild (F) and severe (G) *fzr1* morphants. (**H**) Inf of wild type, *vov* mutant, and mild and severe *fzr1* morphants at 72 hpf. (**I**) Ina for wild type, *vov* mutant and *fzr1* morphant at 72 hpf. (**J-L'**) Confocal images of the lens of 48 hpf wild type (J), *psmd6* morphant (K) and *fzr1* morphant (L) expressing the SAGFF168A; UAS:EGFP transgenes. Individual lens fiber cells are indicated by pseudocolors (J'-L'). (**M**) Individual lens fiber lengths of wild type, *psmd6* morphant and *fzr1* morphant. The average fiber length (horizontal bars) is 50% shorter in both morphants than in the wild type. Scale bars: 50 μm.

Another important question is whether developmental defects outside the lens contribute to the *vov* lens phenotypes. It has been reported that proliferation of lens epithelial cells depends on growth factors (Lovicu and McAvoy, 2005), and as such the *vov*-mediated defects in cell cycle control might be caused by extrinsic factors that emanate from tissues outside the lens. In this study, we found that retinal cell death is suppressed in the *vov*; *p53* double mutant, but that the *p53* mutation does not suppress cell proliferation defects in the *vov* mutant. It seems unlikely that retinal apoptosis is a primary cause of the *vov*-mediated lens defects.

Morphogenesis of lens fiber cells is affected in the *vov* mutant

In this study, we found that nuclear and cell morphogenesis are affected and F-actin density is sparse in the *vov* mutant lens fiber cells. Actin filaments are integral components of the plasma membrane-associated cytoskeleton. Stabilization and remodeling of the membrane cytoskeleton are important for lens fiber differentiation (Lee et al., 2000). The disruption of Rho GTPase activity impairs the organization of actin filaments and lens fiber cell elongation (Maddala et al., 2008). Recent proteome analysis has revealed that ubiquitin is one of the most abundant membrane-associated components of mouse lens fiber cells (Bassnett et al., 2009). These observations suggest that UPS is required for the morphogenesis of lens fiber cells, probably through the regulation of actin filament assembly. It was reported that TGFβ signaling is required for lens fiber differentiation and that the introduction of a dominant-negative TGFβ receptor in the lens results in the inhibition of cell migration and in a failure to assemble F-actin (de Iongh et al., 2001). In the mouse lens, TGFβ signaling promotes APC/C-dependent degradation of the transcriptional co-repressor Sno, which inhibits the transcription of Cdk inhibitors (Wu et al., 2007), suggesting that APC/C mediates the TGFβ-induced cell cycle exit of lens epithelial cells. We found that knockdown of the APC/C regulator Fzr1 induces the nuclear and cell morphogenesis defect of lens fiber cells. These findings suggest that APC/C regulates not only the cell cycle, but also nuclear and cell morphogenesis during lens fiber cell differentiation.

Roles of the UPS in lens denucleation

Denucleation is a characteristic feature of lens fiber differentiation. The degradation of DNA of lens cells depends on DLAD (Nishimoto et al., 2003), suggesting that DNA degradation occurs in an acidic organelle, possibly in the lysosome. This raised the possibility that cellular organelles are degraded by autophagy in the cell's own lysosomes during lens fiber cell differentiation (Nagata, 2005; Nakahara et al., 2007). However, organelle degradation occurs normally in the lens of autophagy-deficient *Atg5* knockout mice (Matsui et al., 2006). In this study, we found that the stage-dependent increases and decreases in lens fiber cell nuclei are altered in the *vov* mutant. A number of lens fiber cell nuclei maintained a plateau between 48 and 60 hpf in the wild type, suggesting a balance between the generation of lens fiber cells and the denucleation of lens fiber nuclei. In the *vov* mutant, the number of lens fiber cell nuclei continued to increase from 48 to 60 hpf, suggesting that the degradation of lens fiber cell nuclei is affected in the *vov* mutant. Furthermore, the fraction of lens fiber cell nuclei located in the anterior half of the lens sphere decreased in the wild type, suggesting that most of the lens nuclei, which are initially positioned in the anterior half region, are degraded. However, a significant number of lens fiber nuclei are retained in the anterior half region in the *vov* mutant. This also supports the idea that denucleation is affected in the *vov* mutant lens fiber cells.

How is the UPS involved in the denucleation processes? Polyubiquitylated proteins are localized in the nucleus of lens fiber cells in zebrafish and mice. GFP-tagged Psmd6 shows a similar spatial localization pattern to the polyubiquitylated proteins, which seems to depend on proteasomal functions. UPS components are localized in the nuclei of bovine differentiating lens fiber cells

(Girao et al., 2005). These observations suggest that a high level of polyubiquitylation occurs in nuclei of lens fiber cells among vertebrates. It is possible that the UPS directly dismantles the nuclear membrane and chromatin from DNA during lens cell denucleation. In the future, it will be important to elucidate the roles of the UPS in lens denucleation.

Acknowledgements
We thank Dr Atsushi Miyawaki (RIKEN BSI, Japan) for providing the zebrafish Cecyil transgenic fish. This work was supported by a Grant-in-Aid from the Ministry of Education, Culture, Sports, Science and Technology to F.I. and a grant from OIST to I.M.

Competing interests statement
The authors declare no competing financial interests.

Supplementary material
Supplementary material for this article is available at
http://dev.biologists.org/lookup/suppl/doi:10.1242/dev.053124/-/DC1

References

Asakawa, K., Suster, M. L., Mizusawa, K., Nagayoshi, S., Kotani, T., Urasaki, A., Kishimoto, Y., Hibi, M. and Kawakami, K. (2008). Genetic dissection of neural circuits by Tol2 transposon-mediated Gal4 gene and enhancer trapping in zebrafish. *Proc. Natl. Acad. Sci. USA* **105**, 1255-1260.
Ashery-Padan, R., Marquardt, T., Zhou, X. and Gruss, P. (2000). Pax6 activity in the lens primordium is required for lens formation and for correct placement of a single retina in the eye. *Genes Dev.* **14**, 2701-2711.
Bassnett, S. (1995). The fate of the Golgi apparatus and the endoplasmic reticulum during lens fiber cell differentiation. *Invest. Ophthalmol. Vis. Sci.* **36**, 1793-1803.
Bassnett, S. and Beebe, D. C. (1992). Coincident loss of mitochondria and nuclei during lens fiber cell differentiation. *Dev. Dyn.* **194**, 85-93.
Bassnett, S. and Mataic, D. (1997). Chromatin degradation in differentiating fiber cells of the eye lens. *J. Cell Biol.* **137**, 37-49.
Bassnett, S., Missey, H. and Vucemilo, I. (1999). Molecular architecture of the lens fiber cell basal membrane complex. *J. Cell Sci.* **112**, 2155-2165.
Bassnett, S., Wilmarth, P. A. and David, L. L. (2009). The membrane proteome of the mouse lens fiber cell. *Mol. Vis.* **15**, 2448-2463.
Berghmans, S., Murphey, R. D., Wienholds, E., Neuberg, D., Kutok, J. L., Fletcher, C. D., Morris, J. P., Liu, T. X., Schulte-Merker, S., Kanki, J. P. et al. (2005). tp53 mutant zebrafish develop malignant peripheral nerve sheath tumors. *Proc. Natl. Acad. Sci. USA* **102**, 407-412.
Bian, Q., Fernandes, A. F., Taylor, A., Wu, M., Pereira, P. and Shang, F. (2008). Expression of K6W-ubiquitin in lens epithelial cells leads to upregulation of a broad spectrum of molecular chaperones. *Mol. Vis.* **14**, 403-412.
Bornheim, R., Muller, M., Reuter, U., Herrmann, H., Bussow, H. and Magin, T. M. (2008). A dominant vimentin mutant upregulates Hsp70 and the activity of the ubiquitin-proteasome system, and causes posterior cataracts in transgenic mice. *J. Cell Sci.* **121**, 3737-3746.
Chow, R. L. and Lang, R. A. (2001). Early eye development in vertebrates. *Annu. Rev. Cell Dev. Biol.* **17**, 255-296.
Collas, P. (1999). Sequential PKC- and Cdc2-mediated phosphorylation events elicit zebrafish nuclear envelope disassembly. *J. Cell Sci.* **112**, 977-987.
Dahm, R., Schonthaler, H. B., Soehn, A. S., van Marle, J. and Vrensen, G. F. (2007). Development and adult morphology of the eye lens in the zebrafish. *Exp. Eye Res.* **85**, 74-89.
de Iongh, R. U., Lovicu, F. J., Overbeek, P. A., Schneider, M. D., Joya, J., Hardeman, E. D. and McAvoy, J. W. (2001). Requirement for TGFbeta receptor signaling during terminal lens fiber differentiation. *Development* **128**, 3995-4010.
Fadool, J. M., Brockerhoff, S. E., Hyatt, G. A. and Dowling, J. E. (1997). Mutations affecting eye morphology in the developing zebrafish (Danio rerio). *Dev. Genet.* **20**, 288-295.
Fanning, A. S. and Anderson, J. M. (2009). Zonula occludens-1 and -2 are cytosolic scaffolds that regulate the assembly of cellular junctions. *Ann. NY Acad. Sci.* **1165**, 113-120.
Finley, D. (2009). Recognition and processing of ubiquitin-protein conjugates by the proteasome. *Annu. Rev. Biochem.* **78**, 477-513.
Fujimuro, M., Sawada, H. and Yokosawa, H. (1994). Production and characterization of monoclonal antibodies specific to multi-ubiquitin chains of polyubiquitinated proteins. *FEBS Lett.* **349**, 173-180.
Girao, H., Pereira, P., Taylor, A. and Shang, F. (2005). Subcellular redistribution of components of the ubiquitin-proteasome pathway during lens differentiation and maturation. *Invest. Ophthalmol. Vis. Sci.* **46**, 1386-1392.
Glasgow, E. and Tomarev, S. I. (1998). Restricted expression of the homeobox gene prox 1 in developing zebrafish. *Mech. Dev.* **76**, 175-178.
Greiling, T. M. and Clark, J. I. (2009). Early lens development in the zebrafish: A three-dimensional time-lapse analysis. *Dev Dyn.* **238**, 2254-2265.
Gross, J. M., Perkins, B. D., Amsterdam, A., Egana, A., Darland, T., Matsui, J. I., Sciascia, S., Hopkins, N. and Dowling, J. E. (2005). Identification of zebrafish insertional mutants with defects in visual system development and function. *Genetics* **170**, 245-261.
Guo, W., Shang, F., Liu, Q., Urim, L., Zhang, M. and Taylor, A. (2006). Ubiquitin-proteasome pathway function is required for lens cell proliferation and differentiation. *Invest. Ophthalmol. Vis. Sci.* **47**, 2569-2575.
Hosler, M. R., Wang-Su, S. T. and Wagner, B. J. (2006). Role of the proteasome in TGF-beta signaling in lens epithelial cells. *Invest. Ophthalmol. Vis. Sci.* **47**, 2045-2052.
Imai, F., Hirai, S., Akimoto, K., Koyama, H., Miyata, T., Ogawa, M., Noguchi, S., Sasaoka, T., Noda, T. and Ohno, S. (2006). Inactivation of aPKClambda results in the loss of adherens junctions in neuroepithelial cells without affecting neurogenesis in mouse neocortex. *Development* **133**, 1735-1744.
Isono, E., Saeki, Y., Yokosawa, H. and Toh-e, A. (2004). Rpn7 Is required for the structural integrity of the 26 S proteasome of Saccharomyces cerevisiae. *J. Biol. Chem.* **279**, 27168-27176.
Isono, E., Nishihara, K., Saeki, Y., Yashiroda, H., Kamata, N., Ge, L., Ueda, T., Kikuchi, Y., Tanaka, K., Nakano, A. et al. (2007). The assembly pathway of the 19S regulatory particle of the yeast 26S proteasome. *Mol. Biol. Cell* **18**, 569-580.
Kiener, T. K., Sleptsova-Friedrich, I. and Hunziker, W. (2007). Identification, tissue distribution and developmental expression of tjp1/zo-1, tjp2/zo-2 and tjp3/zo-3 in the zebrafish, Danio rerio. *Gene Expr. Patterns* **7**, 767-776.
Konishi, Y., Stegmuller, J., Matsuda, T., Bonni, S. and Bonni, A. (2004). Cdh1-APC controls axonal growth and patterning in the mammalian brain. *Science* **303**, 1026-1030.
Kurita, R., Sagara, H., Aoki, Y., Link, B. A., Arai, K. and Watanabe, S. (2003). Suppression of lens growth by alphaA-crystallin promoter-driven expression of diphtheria toxin results in disruption of retinal cell organization in zebrafish. *Dev. Biol.* **255**, 113-127.
Lee, A., Fischer, R. S. and Fowler, V. M. (2000). Stabilization and remodeling of the membrane skeleton during lens fiber cell differentiation and maturation. *Dev. Dyn.* **217**, 257-270.
Liu, Q., Shang, F., Zhang, X., Li, W. and Taylor, A. (2006). Expression of K6W-ubiquitin inhibits proliferation of human lens epithelial cells. *Mol. Vis.* **12**, 931-936.
Lovicu, F. J. and McAvoy, J. W. (2005). Growth factor regulation of lens development. *Dev. Biol.* **280**, 1-14.
Macdonald, R. and Wilson, S. W. (1997). Distribution of Pax6 protein during eye development suggests discrete roles in proliferative and differentiated visual cells. *Dev. Genes Evol.* **206**, 363-369.
Maddala, R., Reneker, L. W., Pendurthi, B. and Rao, P. V. (2008). Rho GDP dissociation inhibitor-mediated disruption of Rho GTPase activity impairs lens fiber cell migration, elongation and survival. *Dev. Biol.* **315**, 217-231.
Masai, I., Lele, Z., Yamaguchi, M., Komori, A., Nakata, A., Nishiwaki, Y., Wada, H., Tanaka, H., Nojima, Y., Hammerschmidt, M. et al. (2003). N-cadherin mediates retinal lamination, maintenance of forebrain compartments and patterning of retinal neurites. *Development* **130**, 2479-2494.
Matsui, M., Yamamoto, A., Kuma, A., Ohsumi, Y. and Mizushima, N. (2006). Organelle degradation during the lens and erythroid differentiation is independent of autophagy. *Biochem. Biophys. Res. Commun.* **339**, 485-489.
McGarry, T. J. and Kirschner, M. W. (1998). Geminin, an inhibitor of DNA replication, is degraded during mitosis. *Cell* **93**, 1043-1053.
Medina-Martinez, O. and Jamrich, M. (2007). Foxe view of lens development and disease. *Development* **134**, 1455-1463.
Murata, S., Yashiroda, H. and Tanaka, K. (2009). Molecular mechanisms of proteasome assembly. *Nat. Rev. Mol. Cell Biol.* **10**, 104-115.
Nagata, S. (2005). DNA degradation in development and programmed cell death. *Annu. Rev. Immunol.* **23**, 853-875.
Nakahara, M., Nagasaka, A., Koike, M., Uchida, K., Kawane, K., Uchiyama, Y. and Nagata, S. (2007). Degradation of nuclear DNA by DNase II-like acid DNase in cortical fiber cells of mouse eye lens. *FEBS J.* **274**, 3055-3064.
Nakayama, K. I. and Nakayama, K. (2006). Ubiquitin ligases: cell-cycle control and cancer. *Nat. Rev. Cancer* **6**, 369-381.
Neuhauss, S. C., Biehlmaier, O., Seeliger, M. W., Das, T., Kohler, K., Harris, W. A. and Baier, H. (1999). Genetic disorders of vision revealed by a behavioral screen of 400 essential loci in zebrafish. *J. Neurosci.* **19**, 8603-8615.
Nishimoto, S., Kawane, K., Watanabe-Fukunaga, R., Fukuyama, H., Ohsawa, Y., Uchiyama, Y., Hashida, N., Ohguro, N., Tano, Y., Morimoto, T. et al. (2003). Nuclear cataract caused by a lack of DNA degradation in the mouse eye lens. *Nature* **424**, 1071-1074.
O'Connell, B. C. and Harper, J. W. (2007). Ubiquitin proteasome system (UPS): what can chromatin do for you? *Curr. Opin. Cell Biol.* **19**, 206-214.
Pesin, J. A. and Orr-Weaver, T. L. (2008). Regulation of APC/C activators in mitosis and meiosis. *Annu. Rev. Cell Dev. Biol.* **24**, 475-499.
Peters, J. M. (2006). The anaphase promoting complex/cyclosome: a machine designed to destroy. *Nat. Rev. Mol. Cell Biol.* **7**, 644-656.

Rupp, R. A., Snider, L. and Weintraub, H. (1994). Xenopus embryos regulate the nuclear localization of XMyoD. *Genes Dev.* **8**, 1311-1323.
Semina, E. V., Ferrell, R. E., Mintz-Hittner, H. A., Bitoun, P., Alward, W. L., Reiter, R. S., Funkhauser, C., Daack-Hirsch, S. and Murray, J. C. (1998). A novel homeobox gene PITX3 is mutated in families with autosomal-dominant cataracts and ASMD. *Nat. Genet.* **19**, 167-170.
Sha, Z., Yen, H. C., Scheel, H., Suo, J., Hofmann, K. and Chang, E. C. (2007). Isolation of the Schizosaccharomyces pombe proteasome subunit Rpn7 and a structure-function study of the proteasome-COP9-initiation factor domain. *J. Biol. Chem.* **282**, 32414-32423.
Shi, X., Luo, Y., Howley, S., Dzialo, A., Foley, S., Hyde, D. R. and Vihtelic, T. S. (2006). Zebrafish foxe3: roles in ocular lens morphogenesis through interaction with pitx3. *Mech. Dev.* **123**, 761-782.
Shiels, A. and Bassnett, S. (1996). Mutations in the founder of the MIP gene family underlie cataract development in the mouse. *Nat. Genet.* **12**, 212-215.
Soules, K. A. and Link, B. A. (2005). Morphogenesis of the anterior segment in the zebrafish eye. *BMC Dev. Biol.* **5**, 12.
Stegmuller, J., Huynh, M. A., Yuan, Z., Konishi, Y. and Bonni, A. (2008). TGFbeta-Smad2 signaling regulates the Cdh1-APC/SnoN pathway of axonal morphogenesis. *J. Neurosci.* **28**, 1961-1969.
Sugiyama, M., Sakaue-Sawano, A., Iimura, T., Fukami, K., Kitaguchi, T., Kawakami, K., Okamoto, H., Higashijima, S. I. and Miyawaki, A. (2009). Illuminating cell-cycle progression in the developing zebrafish embryo. *Proc. Natl. Acad. Sci. USA* **106**, 20812–20817.
Vihtelic, T. S. and Hyde, D. R. (2002). Zebrafish mutagenesis yields eye morphological mutants with retinal and lens defects. *Vision Res.* **42**, 535-540.
Westerfield, M. (1995). *The Zebrafish Book: A Guide for the Laboratory Use of Zebrafish (Danio rerio)*. Eugene, Oregon: University of Oregon Press.
Wigle, J. T., Chowdhury, K., Gruss, P. and Oliver, G. (1999). Prox1 function is crucial for mouse lens-fibre elongation. *Nat. Genet.* **21**, 318-322.
Wu, G., Glickstein, S., Liu, W., Fujita, T., Li, W., Yang, Q., Duvoisin, R. and Wan, Y. (2007). The anaphase-promoting complex coordinates initiation of lens differentiation. *Mol. Biol. Cell* **18**, 1018-1029.
Yamaguchi, M., Tonou-Fujimori, N., Komori, A., Maeda, R., Nojima, Y., Li, H., Okamoto, H. and Masai, I. (2005). Histone deacetylase 1 regulates retinal neurogenesis in zebrafish by suppressing Wnt and Notch signaling pathways. *Development* **132**, 3027-3043.
Zandy, A. J. and Bassnett, S. (2007). Proteolytic mechanisms underlying mitochondrial degradation in the ocular lens. *Invest. Ophthalmol. Vis. Sci.* **48**, 293-302.

Table S1. Morpholino antisense oligos

MO	Sequence (5′ to 3′)	Concentration (mM)
psmd6-MO	CCTCCAGGTTCTCCAAAGGCATTTC	0.2
psmd6-5misMO	CCTCgAcGTTCTCgAAtGcCATTTC	0.2
psmc2-MO	TTCGGTTCCTAAATAATCAGGCATG	1
psmc2-5misMO	TTCGcTTgCTAtATAATgAcGCATG	1
ATG-*fzr1*-MO	CGGCGCTCATAGTCCTGATCCATGG	0.5
fzr1-5misMO	CGGCcCTCATAcTgCTcATCCATcG	0.5
fzr1-splicing-MO	ATTCCAGATGACAGACTAACCATAG	0.5

Mismatches are indicated in lowercase.

Table S2. PCR primers

Gene	Primer	Sequence (5′ to 3′)
psmd6	Forward	GGTGACTGGGACCGGAGG
psmd6	Reverse	ACCTCCAAGATCTCGGCACC
β-*actin*	Forward	GAAATTGTCCGTGACATCAA
β-*actin*	Reverse	GAAGGTGGTCTGTGGATAC